Climate Services 30 (2023) 100385

Contents lists available at ScienceDirect

Climate Services

journal homepage: www.elsevier.com/locate/cliser

Original research article

Projecting China's future water footprints and water scarcity under socioeconomic and climate change pathways using an integrated simulation approach

Yixin Sun [a], Zhuotong Nan [a,b,*], Wendong Yang [a], Longhui Li [a]

[a] Key Laboratory of Ministry of Education on Virtual Geographic Environment, Nanjing Normal University, Nanjing 210023, China
[b] Jiangsu Center for Collaborative Innovation in Geographical Information Resource Development and Application, Nanjing 210023, China

HIGHLIGHTS

- China's water footprints under 52 combined GCM-SSP-RCP scenarios were assessed and projected.
- China's water footprint likely peaks in 2030 and declines thereafter under most scenarios.
- Emission-mitigation measures significantly impact water footprints of electricity.
- Projected water scarcity in China will be most severe in 2025–2035.
- All GCM-SSP2-RCP6.0 simulations show mitigating water stress after 2050.

ARTICLE INFO

Keywords:
Water footprint
Water scarcity
GCAM
Scenario analysis
Socioeconomic and climatic impacts

ABSTRACT

Future changes in climate and socioeconomic systems will exacerbate water scarcity. Previous studies on China's water footprint and scarcity often consider only climate change or socioeconomic factors in isolation. Here, we address these issues by coupling an integrated assessment model, the Global Change Analysis Model, with a global hydrological model to project China's future water footprints and water scarcity, considering both climate change and socioeconomic factors. We simulated China's water footprints under 52 scenarios, which include four global climate models (GCMs) and 13 combinations of Shared Socioeconomic Pathway (SSP)–Representative Concentration Pathway (RCPs) scenarios. We then projected the intensity of water stress (WSI), defined as a ratio of water footprint to renewable water volume, based on the simulations of the SSP2-RCP6.0 scenario. Our results align well with statistical data on water footprint variations between 2005 and 2020. China's water footprints are likely to peak around 2030 and then decrease. We find through a scenario matrix analysis that emission-mitigation measures will significantly impact the water footprint, particularly in the electricity sector, which will become the largest water use sector in the future. This means that the low carbon energy option on China's path to carbon neutrality may aggravate water scarcity. Water stress in China is projected to be greatest in 2025–2035, and all northern basins will experience water scarcity. Projections based on all GCMs consistently show a decline in WSI in China after 2050.

Practical implications

Increasing water scarcity is one of the world's leading challenges, threatening economic development and even human well-being. Climate change and anthropogenic factors, such as population growth, economic development, energy transition and technological improvements, and water management practices, are altering water resources worldwide. As countries take measures to combat climate change, it is crucial to consider the effects of these actions on future water scarcity.

In this study, we developed a methodology that integrates both climate change and socioeconomic developments into a unified

* Corresponding author at: School of Geography, Nanjing Normal University, No.1, Wenyuan Road, Qixia, Nanjing, Jiangsu, China.
E-mail address: nanzt@njnu.edu.cn (Z. Nan).

https://doi.org/10.1016/j.cliser.2023.100385
Received 5 March 2022; Received in revised form 27 February 2023; Accepted 3 May 2023

modeling framework. Our approach enables a comprehensive and synergetic assessment and projection of future water stress in a changing climate context. By using the water footprint approach, we were able to simulate multi-sector water use and environmental demand. The global change assessment model framework accommodates the synergetic effects of climate change and socioeconomic factors on water scarcity. Our results thus provide a link between water management and climate mitigation policies. Given the uncertainties in model structure and inputs, we drew results through a matrix analysis approach based on an array of 52 scenarios covering various climate change, socioeconomic change, and emission mitigation policy options.

Our projections show that China's water stress will be highest in the 2025–2035 period, with most northern basins experiencing water scarcity. Population decline, implementation of water conservation policies, and improvement in water use efficiency explain the mitigation of water scarcity across China by the end of the 21st century. Comparison between scenarios shows that implementation of climate policies is the main cause of differences in water footprint across mitigation scenarios. Actions taken towards emission reduction lead to exacerbation of water use in several sectors, particularly in the electricity sector. The results highlight the importance of considering impacts of climate policies and socioeconomic factors in water management. The results suggest that China's net-zero emission pledge may pose a greater challenge to water management due to the water-intensive nature of many low-carbon energy options, such as unconventional liquid fuels and bioenergy with carbon capture and storage (BECCS). Further water demand resulting from emissions reductions may intensify water scarcity and lead to inter-sectoral and regional competition for limited water supply. When evaluating emission reduction strategies, it is critical to consider whether emission cut measures will increase water demand, which may further escalate competition among water use sectors. In light of the common challenges of water security and the commitment to zero greenhouse gas emissions, the findings of this study can provide policymakers with insights into balancing environmental water demands, socioeconomic development, and emissions mitigation measures.

Data availability

I will share data on figshare and provide a doi to the manuscript.

Introduction

Water scarcity is one of the world's leading challenges, threatening economic development and even human well-being. Two-thirds of global population (4.0 billion people) suffer from severe water stress at least one month per year (Mekonnen and Hoekstra, 2016). According to the AQUASTAT dataset, per capita water availability in China is lower than half the global average (FAO, 2018). China is facing increasingly severe water scarcity, which is an obstacle to economic development (Jiang, 2009, 2015). Climate change affects water scarcity by altering both water supply and demand. Climate change affects the spatial and temporal distribution of water resources, which in turn changes regional water availability (Orlowsky et al., 2014). Additionally, changes in temperature due to climate change affect water use in irrigation and energy sectors (Eom et al., 2012; Konar et al., 2016). In parallel, the human impact on water scarcity cannot not be disregarded. Population and economic development directly increase water demand, while the transition to cleaner energy and advancements in power generation cooling methods and irrigation technologies alter water use efficiency. Furthermore, water management influences water allocation between different sectors and regions (Huang et al., 2021a). At present, many countries are acting to combat climate change. To fully assess the impacts of climate change, it is essential to also consider the impacts of mitigation actions and human adaptation to changing climate (Mendelsohn et al., 1994). Consequently, assessments of water stress must incorporate the combined effects of both climatic and socioeconomic factors (Graham et al., 2020b).

Population, water availability, and water use are common factors used to assess water scarcity. The Falkenmark index (the volume of water available per person) (Arnell, 2004; Falkenmark, 1989) and the water use–availability ratio (Alcamo et al., 2007; Arnell et al., 2011; Graham et al., 2020b) are commonly used to measure water scarcity. However, these methods show only supply-side impacts on water scarcity, without explicit consideration of ecological flow (Liu et al., 2017; Schewe et al., 2014). Hoekstra et al. (2012) developed a water footprint-based method to measure water scarcity by using the ratio of water footprint to water availability. This water footprint approach takes into account ecological flows and water use in various sectors, providing a comprehensive and reasonable assessment of water stress. The water footprint of a product is defined as the amount of water consumed per unit of the product in the production process, i.e., the virtual water content of the product. The water footprint in a geographical unit is thus the sum of the water footprints of all production activities taking place in that unit (Hoekstra, 2009; Tian et al., 2018). Water footprints can be divided into blue, green, and grey water footprints. In this study, we focused on blue water footprints in multiple sectors.

Most studies on water footprint have focused on historical accounting and analysis using statistical data and input–output tables (Xie et al., 2020; Zeng et al., 2012). Several studies have examined climatic impacts and ignored demand-side impacts on water footprint (Konar et al., 2016; Orlowsky et al., 2014). Statistical methods are commonly used in existing studies to project future water footprints based on identified drivers of water footprint such as population and gross domestic product (GDP) (Ercin and Hoekstra, 2014, 2016; Xu et al., 2020; Zhang et al., 2021). This projection approach assumes that the relationship between water footprint and socioeconomic factors will remain constant and valid in the future, which leads to an inadequate consideration of the potential changes in socioeconomic factors such as improvements in water use efficiency, human actions and policy adjustments to water constraints, and coordination among water use sectors. Recently, system dynamics models have been developed to fully account for the influence of socioeconomic factors in projecting water footprint by considering the interactions among water use sectors and water allocation (Feng et al., 2017; Wu et al., 2020). The actual water footprint is affected by both supply and demand sides, but previous studies have often overlooked the constraints imposed by fluctuating water availability. Therefore, a water footprint simulation method that fully considers the synergetic impacts of socioeconomic factors and climate change is needed to better project the future water footprint.

The Global Change Analysis Model (GCAM) is an integrated assessment model based on market-equilibrium theory. GCAM integrates socioeconomics, energy system, land-use change, climate, and water sectors, and provides a mechanism for considering the impacts of socioeconomic factors on water footprint and the interaction between human society and the climate system. In this study, we linked GCAM to a global hydrological model to implement the constraints imposed by the limited supply of natural water resources. We then created 52 scenarios representative of various climate change, socioeconomic change, and emission mitigation policy options, simulated and evaluated water footprint and water scarcity in China through this integrated simulation approach to accommodate the synergetic effects of climate change and socioeconomic factors.

Data and method

Models and dataset

In this study, the water footprint during 2005–2100 was simulated by integrating GCAM and Xanthos. GCAM is an integrated assessment

model based on market-equilibrium theory that includes five modules for socioeconomics, energy, land-use, climate, and water (Calvin et al., 2019). The energy, land-use, and socioeconomics modules calculate the demand for various products and services, and the water module simulates the corresponding water demand in six sectors, including irrigation, electricity generation, industrial manufacturing, mining, livestock, and domestic uses (Kim et al., 2006). The climate module converts radiative forcing into global average temperature, sea-level rise, and other climatic variables, with CO_2 and other greenhouse gas emissions from other modules as inputs. These climatic outputs interact with non-climatic modules, where, for example, decreased temperature can result in growing building heating demand and consequently increasing energy water demand. Through this complex interaction, GCAM provides a more accurate representation of the impacts of both climate change and human activities on water use. GCAM tracks both withdrawals and consumption for each water-use sector (Hejazi et al., 2013). Since actual water use is jointly determined by supply and demand, GCAM constructs a water market to price the balance of water demand and supply at a basin level (Kim et al., 2016). GCAM employs cost resource curves for each basin to determine the share of each of three water sources (e.g., freshwater, groundwater, and desalinated seawater). Typically, surface water is consumed first because it is the cheapest source of water. We used the streamflow simulated by Xanthos as a constraint for surface water availability in a basin. After this renewable water supply is fully depleted, GCAM uses water from the other two sources depending on their relative price. The price of nonrenewable groundwater increases as the volume pumped grows due to the cost of installing and operating the well. Once the price of groundwater rises, desalination becomes more competitive, leading to wider use of desalinated water. GCAM version 5.3 was used in this study and operated in five-year increments with a historical calibration period of 1990–2015 and 2020 as the first projection year.

We used the Xanthos v2.3.1 global hydrological model to simulate basin water availability for historical time periods and future climate change scenarios. Xanthos is an open-source hydrological model developed at the Joint Global Change Research Institute of the Pacific Northwest National Laboratory and written in Python. It is a simplified global hydrological model whose predicative power has been demonstrated in previous studies (Liu et al., 2018). Xanthos divides the global land extent into 235 basins and runs monthly with a spatial resolution of 0.5 geographic degrees (Li et al., 2017; Vernon et al., 2019). The model uses the Penman-Monteith method for potential evapotranspiration, the abcd model for runoff, and the Modified River Transport Model for streamflow routing. Xanthos calculates accessible water supplies for the 235 GCAM basins.

GCAM inputs include data and parameters for historical and future time periods. For the history simulation, the GCAM data system begins with country-level inventory data on energy production and consumption, agricultural production and consumption, land use and land cover, water demand, and emissions. Data and parameters for future periods consist of population (Samir and Wolfgang, 2017), GDP and energy (Dellink et al., 2017), policy and technological assumptions (O'Neill et al., 2017), water efficiency, and technological innovations (Graham et al., 2018). Monthly meteorological data on a global $0.5^\circ \times 0.5^\circ$ grid for the historical period (1950–2005) and future simulations (2006–2100) come from four GCMs (GFDL-ESM2M, HadGEM2-ES, IPSL-CM5A-LR, MIROC5) in the Inter-Sectoral Impact Model Inter-comparison Project (ISIMIP). The meteorological data include key variables such as precipitation, mean temperature, minimum temperature, longwave radiation, shortwave radiation, wind speed, and relative humidity, which are critical in assessing the climatic impacts on water supply. ISIMIP is a subset of the World Climate Research Programme Coupled Model Intercomparison Project -Phase 5 (CMIP5) simulations. The GCMs contained in ISIMIP have a wide coverage of the uncertainty in temperature and precipitation changes projected by 36 CMIP5 GCMs, when compared to otherwise randomly selected GCM subsets (McSweeney and Jones, 2016). The ISIMIP meteorological dataset has thus been used extensively in various studies investigating climate change impacts on water resources (Boulange et al., 2021; Prudhomme et al., 2014; Reinecke et al., 2021; Schewe et al., 2014). Uncertainties associated with climatic inputs and scenario assumptions are discussed in the limitations section.

We used a spatial downscaling algorithm to obtain basin-wide water footprints using population and livestock density maps (Huang et al., 2018; Li et al., 2018). The global population density maps were obtained from the Historical Database of the Global Environment for the period of 1970–1989 and the Gridded Population of the World from the Socioeconomic Data and Application Center for the period 1990–2010, and used for spatial downscaling of four non-agricultural sectors. The gridded global maps of livestock in 2005, produced by the Food and Agriculture Organization's Animal Production and Health Division, were used to downscale livestock water withdrawal. To validate the simulated water footprints, national and provincial water use and withdrawal data in China were extracted from the 2005, 2010, 2015 and 2020 China Water Resources Bulletins (Ministry of Water Resources of China, 2005, 2010, 2015, 2020a).

Study area

The total volume of renewable internal freshwater resources in China is about 281.3 km^3 per year, ranking fifth behind Brazil, Russia, Canada, and Indonesia (FAO, 2018). China's annual per capita water availability is about 1946 m^3, less than half of the global average (FAO, 2018). The distribution of water resources in China is uneven, with the North-South divide expected to worsen due to climate change (Wang and Zhang, 2015). Despite northern China accounting for 65% irrigated land and 45% population, it only has access to 19% of annual renewable water resources. In addition, the rapidly growing population and urbanization in China have led to higher water demand in recent decades.

After spatial discretization and naming in GCAM, we delineated 22 river systems encompassing China's territory as the study area (Fig. 1), with 18 of them draining into oceans and four being interior basins. Among them, 11 river systems that lie entirely within China, including the North Coast of the Bo Hai – Korean Bay (i.e., the Liaohe river basin), Interior Ziya He (a tributary of the Haihe River), Huang He (i.e., the Yellow River basin), Interior Tarim, Interior Plateau of Tibet, Yangtze, Xun Jiang (the middle reaches of the West River, which is the mainstream of the Pearl River), South China Sea Coast (the Pearl River delta, which forms the Pearl River drainage basin by joining with the Xun Jiang basin), the Eastern Coast of China (including the Huai River basin and the southeast rivers), Taiwan (excluding Taiwan Island in this study), and Hainan. These 22 systems also include 11 transboundary basins, i.e., the Hong (Red River), Mekong (Lancang River), Salween, Irrawaddy, Ganges–Brahmaputra (Yarlung Tsangpo River), and the Indus in southern China, the Amur River (Heilong River) in northeastern China, South East Coast of Russia on the northeast coast, Ob River (Ertzis River) in western China, Lake Balkhash, and Interior Gobi in northern China. For these transboundary basins, we applied an area-weighted method to determine the water footprint and water supply within China.

Scenario design

In this study, RCP8.5 was not included in this study due to its unattainable emission target in the GCAM. Simulated streamflow can vary significantly between GCMs, as demonstrated in previous studies (Munia et al., 2020; Schewe et al., 2014). To account for this uncertainty, we used four GCM datasets (GFDL-ESM2M, HadGEM2-ES, IPSL-CM5A-LR, and MIROC5) from ISIMIP-2b (Frieler et al., 2017) for RCP2.6, RCP4.5, and RCP6.0 emission scenarios to project climate change impacts on water resources.

Future socioeconomic scenarios were constructed based on five SSPs and simulated using GCAM. The SSPs include sustainable development

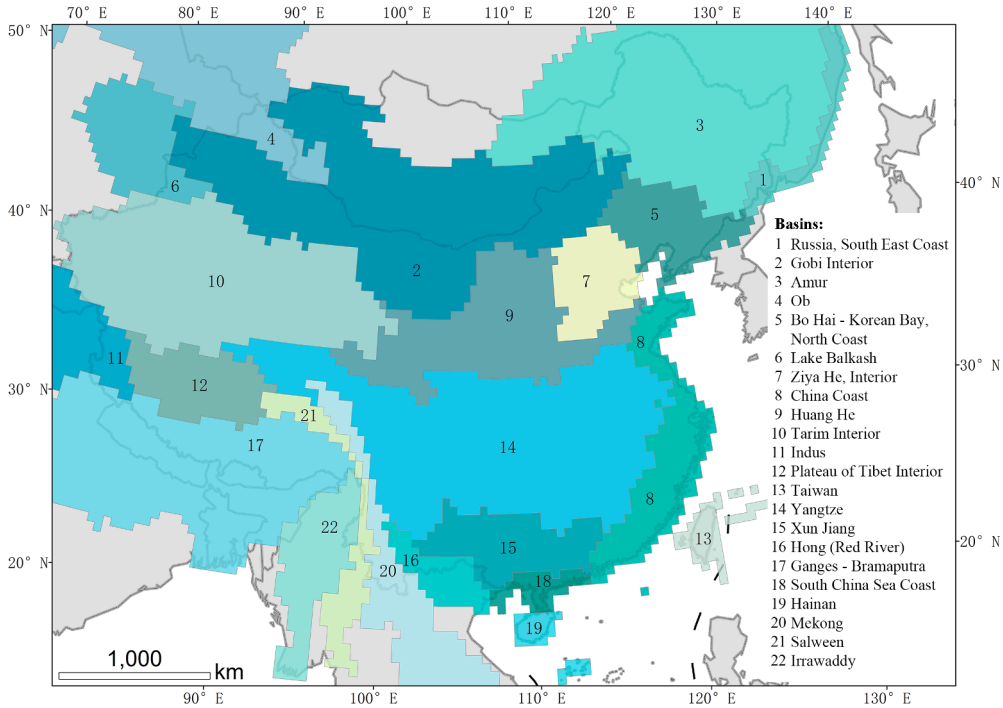

Fig. 1. Division of the 22 river systems encompassing China's territory as the study area. In addition to 11 river basins entirely within China, 11 transboundary river basins (1–4, 6, 11, 16, 17, 20–22) are included, with only the China's parts being considered in this study. The analysis excludes Taiwan Island.

(SSP1), middle-of-the-road development (SSP2), regional rivalry (SSP3), inequality (SSP4), and fossil-fueled development (SSP5) with varying degrees of challenge for climate change mitigation and adaptation. The SSP assumptions comprise qualitative narratives of resource availability, technology developments, and demand drivers such as lifestyle changes, as well as associated quantitative descriptions such as population, economic growth, and urbanization (Riahi et al., 2017). However, the SSPs were developed without explicit assumptions for the water sector. To assess the impact of technological advancement on water footprint, we added assumptions for the water sector following Graham et al. (2018). Qualitative and quantitative assumptions for the future in the water sector include technological advancements and associated efficiency changes in irrigation, electricity generation, industrial manufacturing, and domestic use (Graham et al., 2018). Aligning with economic growth and sustainability assumption in the SSP storylines, SSP1 and SSP5, SSP2 and SSP4, and SSP3 have high to low rates of water technological development. Water-saving cooling systems like dry-cooling are prioritized in electricity sectors. The technological change rate in the municipal and industrial sectors varies across SSPs and regions differing in income level. There are no technological changes in primary energy production and livestock water withdrawal. The specific quantities of withdrawal changes can be found in the work of Graham et al. (2018). Based on demographic and economic drivers and technological improvements, we projected the trajectories of energy use, land use, greenhouse gas emissions, demand for various products and services, and water consumption and withdrawals under various socioeconomic scenarios by employing GCAM's intersectoral connections and feedbacks. For example, regional population and labor productivity assumptions drive the energy and land-use system to produce, transmit, and deliver energy services, as well as crop and forest products, which in turn drives water demand.

Our study produced a total of 52 scenarios based on 13 valid SSP-RCP combinations (Fig. 2) using four GCM outputs. Due to their inability to meet the RCP6.0 emission target by GCAM, we excluded SSP and SSP4 for RCP6.0. Prior to performing the simulations, we had to ensure that the climate change targets in GCAM aligned with the RCP climate targets for Xanthos, which simulated water availability under different climate change trajectories. To this end, we introduced Shared Policy Assumptions (SPAs) which include mitigation and adaptation policies. These assumptions consist of a set of qualitative and quantitative assumptions

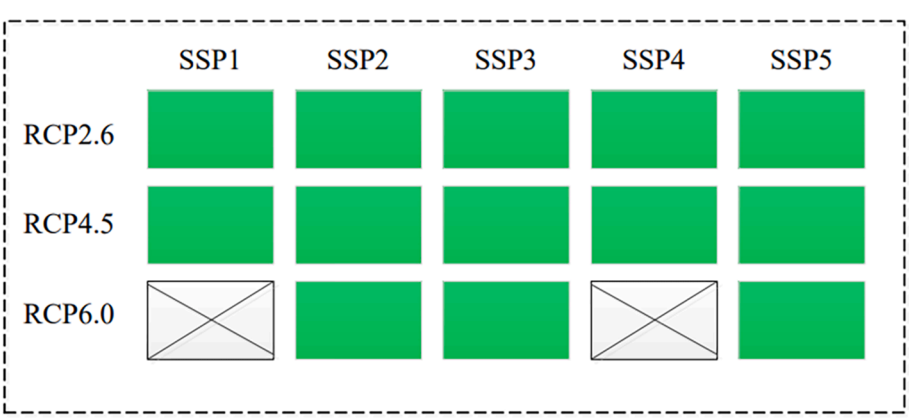

Fig. 2. Scenario matrix consisting of 13 valid combinations of the Shared Socioeconomic Pathway (SSP) and Representative Concentration Pathway (RCP). Based on the Global Change Analysis Model (GCAM) simulations, SSP1 and SSP4 cannot achieve the RCP6.0 emission target. A total of 52 scenarios were created by linking each SSP-RCP combination to four global climate models (GCMs), each providing a possible future climate pathway. Each combined scenario requires varying degrees of climate policy implementation effort to meet the emission target.

about international cooperation and regional distribution of mitigation efforts (Kriegler et al., 2014). By incorporating SPAs into our study, we ensured that the climate change level in both GCAM and Xanthos was consistent. The SPAs vary with the SSPs. SSP1 and SSP4 require low mitigation challenges, SSP5 and SSP3 with high energy intensity require higher mitigation efforts, and SSP2 intermediate mitigation cost compared to the other SSPs (O'Neill et al., 2017). The adoption of SPAs facilitates the mitigation scenarios of SSPs in GCAM to reach the same radiative forcing target of RCPs in 2100 in valid combined SSP-RCP scenarios, allowing both GCAM and Xanthos to simulate under a same CO2 rising level by the end of 2100. In GCAM, climate policies are enforced by levying a tax on greenhouse gas (GHG) emissions as an implementation of the SPA. GCAM calculates the total GHG emissions of each sector subject to the emissions tax, while the climate module determines the corresponding radiative forcing values. GCAM then adjusts the tax amount to find the least cost path to reach the climate target. The start year of the GHG emissions tax varies by SSP, with the tax starting in 2025 in the SSP1 and SSP4 scenarios and in 2040 in the rest SSP scenarios. Beyond taxation, emissions-cutting actions in GCAM also include energy system transformation, such as promoting low-carbon energy (e.g., wind, hydropower, and nuclear), afforestation/reforestation, and reducing the GHG emission intensity of agriculture. We collected radiative forcing in 2100 under five SSP baseline scenarios from Calvin (2017) (5.6 W/m^2 in SSP1 baseline, 7.5 W/m^2 in SSP2 baseline, 7.2 W/m^2 in SSP3 baseline, 6.4 W/m^2 in SSP4 baseline and 8.4 W/m^2 in SSP5 baseline). By comparing the baseline radiative forcing and the RCP target, we can roughly estimate the difficulty of attaining the target prescribed in each combined SSP-RCP scenario through mitigation measures. For example, among SSP3 scenarios, SSP3-RCP2.6 requires higher mitigation costs than SSP3-RCP4.5 or SSP3-RCP6.0.

We investigated the impacts of climate policy and climate change on water footprint with the aid of scenario matrix. It is important to note that not all of scenarios have equal probability of occurrence, as those with high mitigation cost are less likely to occur. As shown in Fig. 2, each column of the matrix represents scenarios with different RCP targets under the same SSP assumptions, with variations within each column reflecting the impacts of both mitigation measures and climate change on water footprint. Each row of the matrix represents scenarios under different SSPs with the same RCP, with variations within each row indicating the socioeconomic contribution to water footprint.

Water footprint and water scarcity indicator

Water footprint is used to evaluate water consumption. The water scarcity index (WSI), defined as a ratio of water footprint and accessible water volume, is used to assess water stress. The accessible water volume, based on the Xanthos simulation, is the minimum value between the streamflow and the sum of the baseflow and reservoir storage (Kim et al., 2016). The amount of water needed to maintain ecological use, known as the environmental flow requirement (EFR), was estimated to be 10 % of the monthly mean natural streamflow (Kim et al., 2016) and was subtracted from natural streamflow in each basin. The total reservoir storage volume for each basin was taken from the Global Reservoir and Dam Database (Lehner et al., 2011), and the volume was assumed constant over time in this study. The accessible water volume in each basin was then used as a constraint on water supply in GCAM (Graham et al., 2020b).

The national water footprints include the water footprints of two agricultural and four non-agricultural sectors. In this study, we followed the definitions of water consumption and water withdrawals of Hejazi et al. (2014) to reconcile with GCAM. The non-agricultural water footprint refers to water consumption in four sectors: electricity generation, industrial manufacturing, mining, and domestic use (Mekonnen and Hoekstra, 2016). The agricultural water footprint refers to water withdrawals for irrigation and livestock. To facilitate evaluation of future progress in water use efficiency, we define water footprint in agricultural sectors on the basis of water withdrawals, which are the water diverted or withdrawn from a surface water or groundwater source. Compared to water withdrawals, agricultural water consumption accounts for crop evapotranspiration and livestock consumption, but ignores other water losses such as irrigation evaporation and those during transport, resulting in an underestimation of agricultural water footprint and a failure to account for technological advances in water use efficiency. However, one potential drawback of using water withdrawals is a lack of consideration of return flows, which are very difficult to track. To mitigate this effect, we subtracted a minimal amount of EFR from the denominator of WSI when evaluating water stress.

By linking GCAM and Xanthos, we simulated national water withdrawals and consumption for the six sectors at a 5-year time step over the period of 2005–2100, as well as water withdrawals for irrigation at the basin level. Water withdrawal for irrigation in each basin is considered as the agricultural water footprint, national water withdrawal for livestock is considered as the national livestock water footprint, and national water consumptions for electricity generation, industrial manufacturing, mining, and domestic sector are considered as national water footprint of each sector. The national water footprints of six sectors are aggregated to obtain the water footprint in China. For the non-agricultural and livestock sectors (i.e., electricity generation, industrial manufacturing, mining, and domestic uses), gridded water footprints (0.5°) were first obtained by downscaling national footprints of those sectors based on population or livestock density maps, and then aggregated to obtain basin-wide water footprints for the respective sectors (Li et al., 2018).

A basin is considered to be affected by water stress if the WSI value is greater than 0.4, i.e., the water footprint exceeds 40% of the accessible water resources (Falkenmark et al., 2007). Among all the valid SSP-RCP scenarios, SSP4-RCP2.6, SSP5-RCP2.6, and SSP5-RCP4.5 are unusual because of the high costs associated with achieving stringent climate goals, as reflected by the large gaps between SSP baseline estimates of radiative forcing and RCP targets. SSP2-RCP6.0 is a scenario with minimum mitigation costs (Fricko et al., 2017; van Vuuren et al., 2014). In SSP2 ("Middle-of-the-road") scenarios, future socioeconomic conditions evolve along the current pathway, such as steady population and economic growth and fixed energy and fuel preferences. The SSP2-RCP6.0 scenario is frequently used to assess water scarcity in existing studies (Huang et al., 2021a). Thus, we also focused on the results of the SSP2-RCP6.0 scenarios to facilitate comparisons with other studies.

The simulated national water footprints were verified with statistical data from the China's water resources yearbooks. In addition, the downscaled water footprints of a 0.5° resolution were aggregated to the provincial level and compared with provincial statistical data.

Results

Changes in China's water footprint

The national water footprint in China, calculated as the mean of all scenario simulations, has increased over the historical period (2005–2015) in a similar trend to the statistical data, with a Pearson correlation coefficient of 0.96 and a mean absolute percentage error of about 6.0% relative to the statistical data (Fig. 3a). While the simulation results in 2005 underestimated the national water footprint by about 10.3%, the simulated water footprint in 2020 was 14.2% higher than the statistical data. Our model did not account for many unexpected factors that together resulted in a reduced water consumption in industry, agriculture and households in 2020, such as the effects of COVID-19 pandemic and a 10% increase in annual precipitation compared to the multi-year average (Ministry of Water Resources of China, 2020b). It is intriguing that our simulation shows a steady increase in national water footprint over the 2005–2020 period, whereas statistical data show a peak in 2013. Zhao et al. (2021) have raised doubts about the validity of the turning point in 2013, given that China's water consumption did not

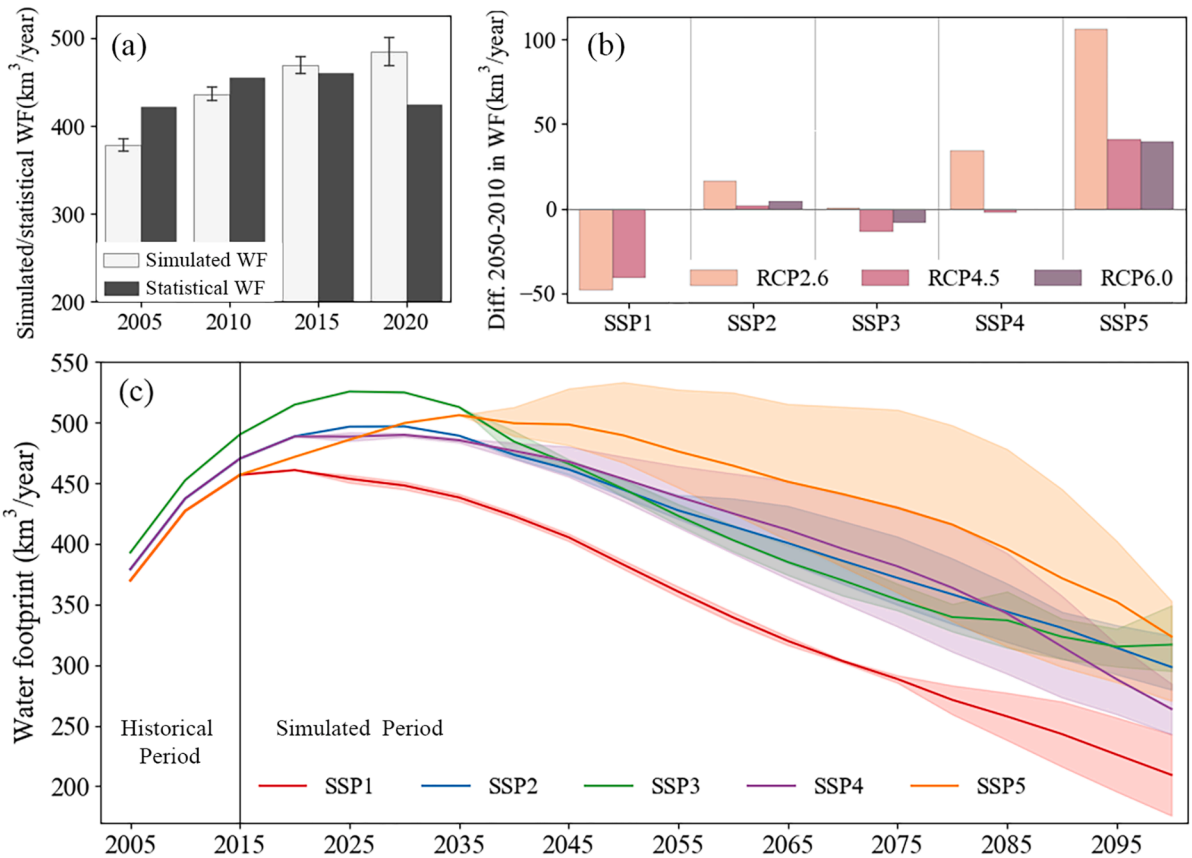

Fig. 3. Simulated national water footprints (WF) in China during 2005–2100 under SSP1-SSP5. (a) Bar chart showing the simulated national WF and the WF from the statistical data in 2005–2020. The gray bars represent the mean of 52 simulations results, and the error bars represent a 95% confidence. (b) Differences in water footprint between 2050 and 2010 under 13 SSP-RCP combined scenarios. This subplot is to contrast with the results from Xu et al. (2020) which also calculated the differences over this time interval. For each SSP-RCP scenario, the mean value is plotted based on four GCMs. (c) Changes in China's annual water footprints based on the simulation results under the total 52 scenarios. The solid lines show the mean values and the shaded band shows the range of all GCM-RCP simulations under each SSP.

reach a peak in that year referring to economic development. Their study suggested that the total water use in China would likely reach its maximum in 2035–2040. The reasons behind the occurrence of the turning point in 2013 are multifaceted (Zhao et al., 2021). One possible reason is related to statistical methodology. In 2010–2012, China conducted the first national water census and reported an industrial water consumption of 120.3 km^3 in 2011. This was 25.9 km^3 lower than the industrial water consumption in the China Water Resources Bulletin for the same year. As a result, the statistical data of the bulletin was corrected from 2012 onwards by a bias correction procedure. In 2012, a red line was set for water resource use in China, imposing a cap of 700 km^3 by 2030. While this regulation encourages the development and application of water saving technologies, it can also provide incentives for local authorities to report less than their actual water consumption.

On average across all scenarios, China's simulated water footprint increased from 378.7 ± 2.4 km^3 (with a 95% confidence level, CL) in 2005 to a maximum of 501.2 ± 6.1 km^3 (95% CL) and later decreased to 289.4 ± 13.2 km^3 (95% CL) in 2100 (Fig. 3c). However, the magnitude and timing of the maximum water footprint varied for individual SSPs, with maxima ranging from 460.9 km^3 to 525.6 km^3 across all 52 scenarios (Fig. 3c). In particular, under the SSP5 scenarios, the national water footprint peaks in 2035–2050, while the peak values under all scenarios except SSP5 are likely to occur before the 2030 s. Under the SSP1 scenarios, the water footprint peaks as early as the 2010 s. In the SSP2, SSP3, and SSP4 scenarios, the water footprint peaks in 2020–2025. In SSP3 and SSP5, the water footprint peaks at over 500 km^3. High energy demand and steady GDP growth contribute to the delayed and higher peak under the SSP5 scenarios. The high population in SSP3 also results in a high peak water footprint. The peak values are relatively lower in the SSP2 and SSP4 scenarios, with a value of about 491.9 km^3. The lowest peak value appears in the SSP1 scenarios (460.9 km^3). The decrease in water footprint after the peak is likely due to population decline, which is an input variable for GCAM. China's water footprint in 2050 is either lower than or closer to the water footprint in 2010 under all but the most energy-intensive SSP5 scenarios (SSP5-RCP2.6, SSP5-RCP4.5, SSP5-RCP6.0) and the RCP2.6 scenarios with the lowest emissions (e.g., SSP4-RCP2.6 and SSP2-RCP2.6) (Fig. 3b). In contrast, Xu et al. (2020) arrived at the opposite conclusion that the water footprint in 2050 is much higher than in 2010 under all SSP1-5 scenarios. The disparity can be attributed to the fact that Xu et al. (2020) considered only socioeconomic factors without natural water constraints.

As shown in Fig. 3c, the water footprints under the same SSP assumptions (e.g., SSP2-RCP2.6, SSP2-RCP4.5, SSP2-RCP6.0) begin to diverge after the introduction of a GHG tax. In GCAM, the baseline year for GHG taxation is 2040 in SSP2, SSP3, and SSP5, and 2025 in SSP1 and SSP4. The divergence suggests that climate policy implementation is the main reason for the differences in water footprints under the same SSP assumptions. According to our simulation, the scenarios with stringent climate targets (such as RCP2.6) lead to high water footprints in the GHG-taxed years (Fig. 3b, Table A.1). Under the same SSP, the simulated water footprints in the RCP2.6 scenarios are higher than those in the RCP4.5 scenarios by 2080, and in both the RCP2.6 and RCP4.5 scenarios, they are significantly higher than those in RCP6.0. For example, under the same SSP5 settings, the water footprint in the SSP5-RCP2.6 scenario is over 100 km^3 larger than those under the other SSP5-RCP

scenarios. This large difference in water footprint is in line with the assumption that achieving an RCP2.6 target in SSP5 requires high mitigation costs (Kriegler et al., 2017). The water footprint in SSP4-RCP2.6 is also larger than that of SSP4-RCP4.5 by about 50 km^3 for the period of 2055–2095, which is half the difference observed in the corresponding SSP5 scenarios. Note that the water footprint in SSP4-RCP4.5 is ranked as the fourth highest of all RCP4.5 scenarios, while the water footprint in SSP4-RCP2.6 is ranked as the second highest of all five RCP2.6 scenarios. Therefore, lower mitigation costs are required under SSP4 to achieve the RCP4.5 emissions target than under the other SSP scenarios, but costs increase substantially to achieve the RCP2.6 target under SSP4, as also noted in Calvin et al. (2017).

China's water footprint by sectors

Similar growth and drawdown trajectories of water footprint in China are projected under all scenarios for the 21st century, but the causes behind them are different. The late decline in national water footprint in all SSP scenarios except SSP3 is mainly due to the reduction of water footprint in the industrial and domestic sectors, while the decline in SSP3 is caused by the reduction of water footprint in the electrical and domestic sectors (Fig. 4). The projected water footprints by sectors for all scenarios are presented in Table A.2. In 2005, water footprints in irrigation, industry, domestic use, and electricity sectors account for about 90% of the national water footprint. In most scenarios, the share of the water footprint for electricity generation and irrigation increases over time, while the share of the water footprint for industry, domestic use, livestock, and mining decreases. By 2100, irrigation, electricity, and industry become the most important sectors of the water footprint. The water footprints in the livestock, domestic use, and mining sectors increase and then decrease, reaching a reversal point in 2015, 2020, and 2035, respectively.

The domestic water footprint decreased since 2015 in SSP3 scenarios, despite the peak population expected in 2030. This indicates the positive impact of technological advances on offsetting the increase in water demand resulting from population growth. Similarly, in SSP1 scenarios where population peaked in 2020, the domestic water footprint peaked as early as 2015. Zhou et al. (2020) have also emphasized the role of technological advancement and water conservation measures in offsetting the increase in the water demand resulting from socioeconomic development. Interestingly, despite the different population projections in SSP1 and SSP3, both scenarios exhibit a declining trend in domestic water footprint during 2030–2100 (Fig. 4), highlighting the critical role of technological improvement in driving down the domestic water footprint. However, by 2100, the domestic water footprint in SSP3 remains larger than that in SSP1, though with a diminishing difference (Table A.2). This implies that population continues to exert influence on domestic water footprint.

The irrigation, industry, and electricity sectors are the primary drivers of variation in water footprints across the different SSPs. In most scenarios, irrigation water footprints grow until 2030 and drop thereafter. In SSP3, the irrigation water footprint grows steadily and reaches 160 km^3 in 2050, which is 60% higher than other scenarios in the same year. This high irrigation water footprint is attributed to the large population and slow advancement in irrigation efficiency in SSP3 assumed in GCAM. In particular, China's population in SSP3 is nearly twice that in SSP1 by 2100. The industrial water footprint is projected to grow through 2030 before declining in most scenarios, albeit peaking in the 2010s in SSP1. The water footprint for electricity generation varies significantly by SSP. It increases substantially over time in the SSP2, SSP4, and SSP5 scenarios, whereas in SSP3 it tends to decrease. For the three remaining sectors (i.e., livestock, domestic use, and mining), water footprints are of a similar magnitude across the five SSPs. Across all sectors, the water footprint in 2100 is smaller than in 2005, except for the electricity sector.

Upon examining the simulations for the same SSP (column-wise in Fig. 4), one can see that the water footprint response to each climate change mitigation target varies by sector, with the electricity sector contributing the most, followed by the irrigation and industry sectors. The water footprints of the three remaining sectors (i.e., livestock, mining, and domestic use) are almost identical across the different climate mitigation scenarios (Fig. 4). The difference between SSP4-RCP2.6 and SSP4-RCP4.5 in the total water footprint is +41.7 km^3 in 2100, while the difference in water footprint for electricity generation is +45.2 km^3. Similarly, the total water footprint difference between SSP1-RCP2.6 and SSP1-RCP4.5 is +67.1 km^3, with electricity accounting for

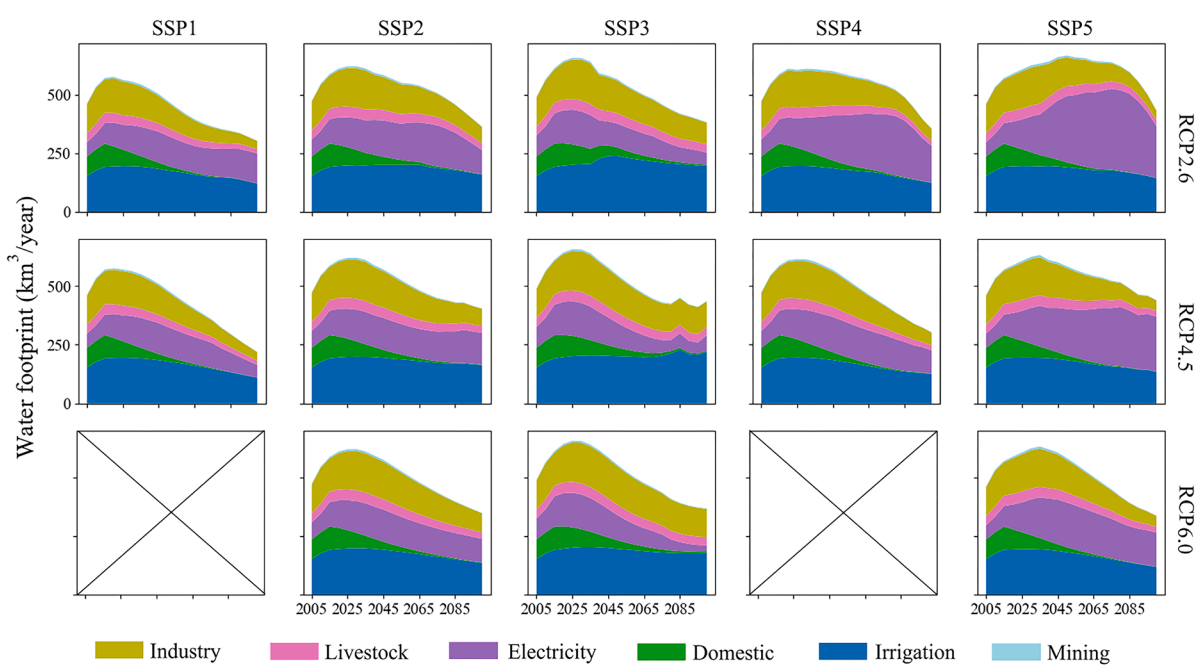

Fig. 4. Projected national water footprints by sector across 13 SSP-RCP scenarios. SSP1-RCP6.0 and SSP4-RCP6.0 are invalid scenarios as the RCP6.0 emissions target in SSP1 and SSP4 cannot be achieved by GCAM. The water footprints shown in the subplots are averages based on four GCMs associated with each SSP-RCP scenario.

+59.4 km^3. The water footprints in the electricity and irrigation sectors appear to be larger under the stringent climate policy scenarios (RCP2.6 and RCP4.5). However, the industrial sector shows a contrasting result, with a small water footprint under the stringent climate policy scenarios.

China's future water scarcity trend

We estimated future water scarcity in China based on simulations under the four SSP2-RCP6.0 scenarios applying different GCM climate projections. The percentage changes in WSI averaged over the four GCM projections are shown in Fig. 5. It shows that the national WSI initially increases and later decreases during the study period (2005–2100). The average national WSI is 0.286 in 2005 and about 0.345 in 2020–2035. Subsequently, it falls steadily to 0.184 by 2100, indicating a reduction in water stress in China compared to 2005. Based on estimates, most basins will experience their peak water stress in 2035. Fig. 5 shows that in the Amur and Huang He basins, WSI is likely to peak in 2020, while in the Yangtze basin and the interior Ziya He basin, it is likely to peak in 2025. The Xun Jiang basin and South China Sea Coast will reach their peak WSI around 2030, while the Eastern Coast of China will continue to experience an increase until it peaks in 2055. The most severe water scarcity in China varies in terms of timing and intensity across the GCM-SSP2-RCP6.0 scenarios. The national average WSI peaks at 0.365 in 2035 for GFDL-ESM2M, 0.350 in 2030 for MIROC5, 0.350 in 2025 for HadGEM2-ES, and 0.377 in 2025 for IPSL-CM5A-LR. In other words, the most severe water stress in China will occur in 2030s, with a national average WSI of 0.360 ± 0.010 (95% CL). It is worth noting that all four GCM-SSP2-RCP6.0 simulations consistently show that water stress at the national scale in China will steadily decrease after 2050. For a detailed view of the estimated WSI trajectories in all 22 basins in China and the national mean, the reader is referred to Fig. A.1.

In general, water stress in China is highest around 2035 under the SSP2-RCP6.0 scenarios (Fig. 6). In 2035, most northern basins experience water shortage, and the WSI values of five northern basins exceed 0.4, including the interior Ziya He basin (2.13), Huang He basin (0.87), East China Coast (0.78), Liaohe river basin (0.5) and the interior Gobi (0.47). In particular, the water footprint in the interior Ziya He basin is more than twice the available water in the basin. In addition, water stress in the South China Sea Coast (0.38) is higher than the national average (0.33) in 2035, and these five northern basins will continue to face water scarcity in mid-century. By 2075, water scarcity will no longer exist in the interior Gobi and Liaohe river basin. By the end of the century, the nationwide mean WSI will drop to 0.19, but three basins will still surfer water scarcity: the interior Ziya He basin (1.25), East China Coast (0.56), and the Huang He basin (0.47).

Almost all basins experienced intensified water scarcity under the SSP2-RCP6.0 scenarios during the historical period (2005–2015) (Fig. 6d). The WSI change rates in the interior Ziya He basin, Bo Hai and Huang He basins were all less than 10%, while other basins experienced a change rate of more than 10%, such as the Yangtze (22.8%), Indus (44%), and interior Gobi (39%). Half of the 22 basins are likely to receive moderate reductions in water stress, with a rate of change less than 5% over the 2015–2035 period (Fig. 6e). By contrast, some basins are exposed to even more severe water stress over this period, with an increase of about 10% in WSI, such as the East China Coast, Pearl River, Bo Hai. In all basins, water stress will decrease in 2100 compared to 2035, with a decreasing rate of change close to or above 30% (Fig. 6f). The negative changes in WSI will be more than 50% between 2035 and 2100 in Interior Tarim, and Interior Plateau of Tibet. It's worthy to note that in these basins, the WSI remain below 0.1 in all scenarios, due to the small water footprints resulting from the low levels of production and population in these areas of our study.

Discussion

Comparison with previous studies

Our analysis shows that the water footprint in China is likely to peak around 2030 and then decline as simulated under most scenarios, which is consistent with the results of previous studies on water use in China. For instance, Zhao et al. (2021) projected that total water use in China would reach a turning point in 2035–2040, due to demand-side economic development and water management such as improved water efficiency, conservation measures, and water supply constraints. A recent study based on historical water use data in China also supports the future declining trend in water use, noting that both technological advancement and water conservation measures offset the increase in water demand caused by socioeconomic development (Zhou et al., 2020). However, there is still no consensus on the future trend of national water footprints. Xu et al. (2020) reported that the national water footprint in China would increase significantly in the future for all five SSPs throughout 2010–2050. Our study differs from Xu et al. (2020) in that we considered water supply constraints and water efficiency improvements, which Xu et al. did not. On the other hand, based on the statistical data, some studies suggested that water consumption would continuously decline in the future. Zhang et al. (2021) inferred from the historical water use data that China's water consumption crested in 2013 and would continuously decrease in the period 2013–2030 by using the Logarithmic Mean Divisia Index method and the Monte Carlo method, but the reliability of their findings was questioned due to uncertainty around the peak in 2013 according to Zhao et al. (2021). More importantly, the statistical method has limitations as it relies on the

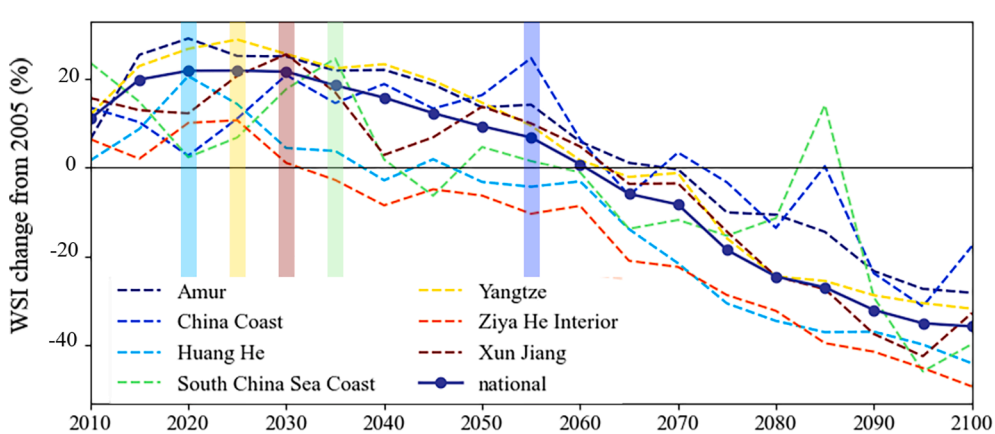

Fig. 5. Percent changes in water scarcity index (WSI) relative to the 2005 level, both nationwide and in seven basins with the highest WSI values over 2010–2100. The values are averages based on four SSP2-RCP6.0 scenarios with different GCM projections. The bars specify the year of the occurrence of the highest WSI values of the basins in the corresponding colors.

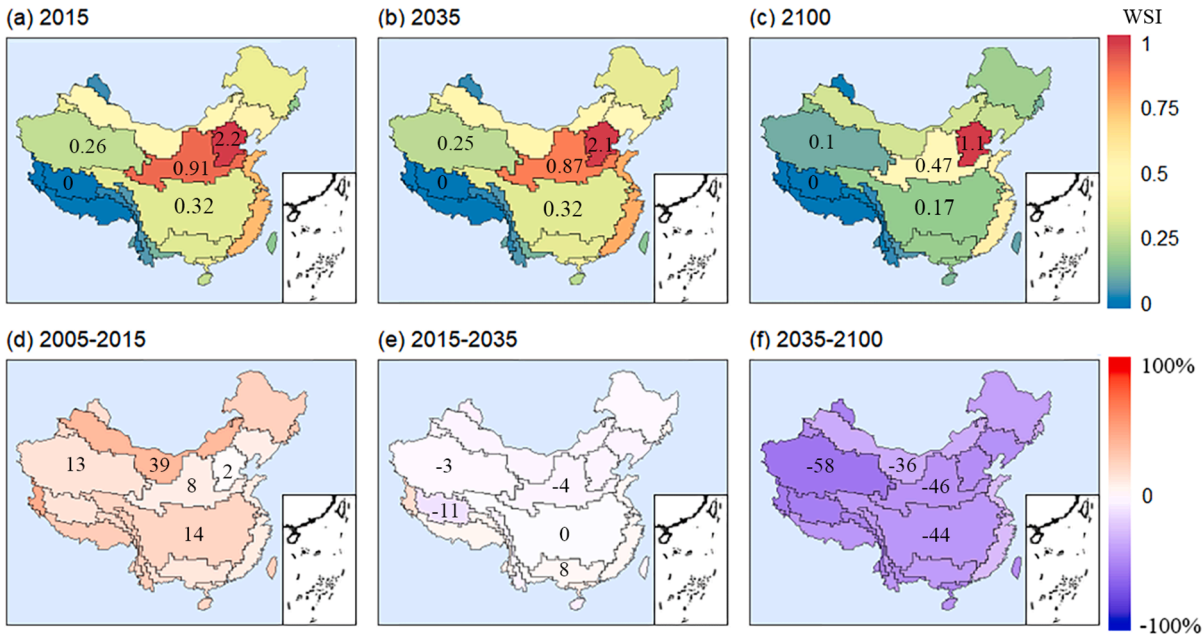

Fig. 6. Water stress estimates in China in 2015 (a), 2035 (b), and 2100 (c) and normalized relative percent changes in WSI between 2005 and 2015 (d), 2015–2035 (e), and 2035–2100 (f). WSI values are calculated as averages of four GCM-SSP2-RCP6.0 simulations. Yellow and red colors indicate water stressed basins. Relative percent changes in WSI are presented as normalized values using a Min-Max approach with the values from all basins. A negative normalized relative percent value indicates an improvement in water stress relative to the reference year (e.g., 2005 in (d)), while a positive value indicates a worsening of water stress. (For interpretation of the references to colour in this figure legend, the reader is referred to the web version of this article.)

relationship between water use and factors like economic development and historical industrial structures. It often overlooks the intricate interactions between socioeconomic factors and water use. Moreover, this method assumes a constant relationship that may not hold true in the future, which could impede its ability to project future water use.

Our simulated water scarcity states in China for 2005 and 2010 align with previous studies (Ge et al., 2016; Greve et al., 2018; Liu et al., 2017). Several studies have used GCAM to assess future global water scarcity in light of various climatic and socioeconomic factors (e.g., Graham et al., 2020a; Huang et al., 2021b). Other regional studies have projected water use based on demand and water constraints. For example, Smolenaars et al. (2022) projected water use in the Indus basin under consideration of various climatic and socioeconomic factors while accounting for inter-basin variability in water supply. Our study specifically focuses on water scarcity issues in China. The results of our analysis align with global projections that northern China will endure water scarcity in this century and that China can expect less water stress at the end of century than in 2005. We also highlight the finding that China will face the worst water scarcity in 2025–2035, which has never been previously reported in global studies. We attribute the decline in water stress after 2050 to technological improvements, energy shifts, and population decline in China. Unlike previous studies, we projected the future WSI changes based on four GCM outputs, which enhances confidence in our finding that the national water stress in China will decline in the late 21st century.

Implications to the pathways to carbon neutrality

Different water footprints simulated under the same SSP assumptions reflect the impacts of emission mitigation measures in climate policy scenarios. This study has indicated that emission reductions often come at the cost of high water footprint. Many emission cut actions exacerbate water use in several sectors, particularly the electricity sector, as previous studies have found (Fricko et al., 2016; Kyle et al., 2013).

China has committed to peaking its emissions before 2030 and becoming carbon neutral by 2060. In this context, a low carbon energy transition is needed to balance the promise of reducing emission and satisfy growing energy demand. Meanwhile, China has set a national water use goal that annual water consumption must not exceed 700 km^3 by 2030. Given the dual constraints (carbon emission and water use), energy decisions should be made wisely. Many low-carbon energy options are water-intensive. While existing studies suggest that bioenergy with carbon capture and storage (BECCS) is a feasible carbon-negative technology (e.g., Azar et al., 2010), the irrigation of energy crops for biomass production leads to higher water consumption than fossil fuels and undermines food security (Séférian et al., 2018). The shift from conventional oil to unconventional liquid fuels also increases water demands (Clark et al., 2013). The large-scale deployment of low-carbon, water-intensive technologies would significantly increase water demand and result in a potential water crisis. Although Direct Air Capture, a negative emission technology, uses less water than BECCS (e.g., Madhu et al., 2021), the technology is still at a preliminary research stage and has not yet demonstrated its applicability on a large scale (Madhu et al., 2021). Hydrogen is also a clean energy source with no GHG emissions and uses less water. However, several problems impede the widespread application of hydrogen energy. Currently, most hydrogen is generated from fossil fuels rather than expensive renewable energy and natural gas (IEA, 2021). Researchers also note that hydrogen leakage could indirectly cause global warming by extending the lifetime of methane and other GHGs in the atmosphere (Derwent et al, 2020).

Further water demand arising from emission reductions could intensify water scarcity and lead to regional water competition. To avoid this problem, sustainable water management policies are imperative as part of regional regulation. To fundamentally solve this problem, low-carbon and low water-intensity energy sources such as wind and solar photovoltaics must be sought, and water-efficient cooling technology for power plants must be promoted. Studies have shown that air and seawater cooling technologies can effectively reduce water use for power generation and reduce water demand by 50–80% (Fricko et al., 2016; Kyle et al., 2013). When assessing emission reduction strategies, it is critical to consider whether the measures increase water demand, which can intensify competition among water use sectors. Further

research is necessary to demonstrate how to balance environmental water demand, socioeconomic development, and emission reduction measures.

Limitations

National water use in China is strongly influenced by policy regulations, yet this study has limitations as it does not consider water-related policies that directly affect water footprints, except for emission mitigation and adaptation policies. Furthermore, the new "three-child policy" in China, aimed at increasing birth rates, will directly increase water demand but was not considered in this study. In addition, transboundary water allocations result in water resource redistribution. The South-North Water Diversion Project, which moves surplus water from water-surplus basins to water-scarce basins, affects water supply in China (Yin et al., 2020) and alleviates stress condition, but may reduce ecological water supply and undermine watershed environment. Our study did not consider the impact of global trade on regional water footprints through the transfer of water-intensive products such as wheat and rice (Muratoglu, 2020). Graham et al. (2020) found that agricultural trade leads to significant virtual water flows between regions, which may lead to discrepancies between projected results and actual water use.

While our estimation accounts for technological improvements in the electricity, agriculture, and industry sections, the water market applies to a basin level, so the differences in water supply systems and water infrastructure within a large basin cannot be considered. This simplified setting may not fully reflect the real China. For example, water-efficient irrigation is rarely used in water abundant regions like southern China where terrace farming is practiced. In addition, the treatment and reuse of wastewater increases water supply, but recycled wastewater was not included as a water source in this study.

The choice of hydrological and climatic models has been shown to influence the simulation of water stress (Schewe et al., 2014). While we used data from multiple climate models, we relied on a single hydrological model, which may introduce uncertainties in predicting runoff. Notably, our research focused on watersheds that are much more finely gained than the national scale typically used in many water scarcity research. We applied a simple downscaling/upscaling approach to allocate water to and from catchments, but even this has uncertainty, especially in the treatment of transboundary water allocation for international catchments. In large basins, upstream water use has a bearing on downstream water scarcity. Previous research has found that human activities exacerbate downstream water scarcity through water withdrawal and wastewater discharge (Veldkamp et al. 2017).

This study explicitly considered ecological water demand and, as per Kim et al. (2016), we used 10 % of the long-term mean monthly natural streamflow as the EFR. However, the EFR varies from basin to basin, and the 10% threshold is close to the low end of actual EFR (Hogeboom et al., 2020; Voisin et al., 2013), which ensures minimal ecological conservation. Therefore, incorporating basin-specific EFR values in the WSI calculation may provide a more realistic estimate of water stress.

Conclusions

In this study, we developed an integrated modeling approach to simulate water footprints and water scarcity in China, which allows for the simultaneous consideration of climate change and socioeconomic factors. We integrated the global hydrological model Xanthos with the integrated assessment model GCAM to provide available water supply and constrain GCAM. We evaluated future changes in water footprint in China from 2005 to 2100 under different climatic and socioeconomic conditions using 52 GCM-SSP-RCP scenario combinations, and then assessed water scarcity in 22 basins of China under SSP2-RCP6.0.

Our results show that the established integrated modeling approach can well reproduce historical water footprints. China's water footprint peaks in 2030 s during 2005–2100 and then declines steadily under all scenarios except the SSP5 scenarios. The simulated mean water footprint of China can be as high as 501.2 ± 6.1 km^3 (95% CL) before decreasing to 289.4 ± 13.2 km^3 (95% CL) in 2100. With all scenarios considered, the maximum national water footprint can range from 460.9 km^3 to 525.6 km^3. The electricity and domestic sectors in SSP3 and industrial and domestic sectors in the other SSPs lead to a reduction in the national water footprint. While irrigation and industry are the two most important water use sectors in 2005, irrigation and electricity become the most important in 2100. The water footprint for electricity generation grows significantly in the SSP2, SSP4, and SSP5 scenarios, making electricity one of the most important water use sectors in 2100. Analysis of the scenario matrix indicates that climate policy implementation is the main reason for variations in the water footprint across climate mitigation scenarios. Emission reductions in the electricity sector have a strong impact on the water footprint, and the implementation of stringent climate policies increases the water footprint of electricity generation.

In general, water stress in China is highest in 2030s with a national average WSI of 0.360 ± 0.010, and most northern basins experience water scarcity in these years. The water footprint in the interior Ziya He basin is more than twice the available water. The SSP2-RCP6.0 projections based on four GCM outputs consistently show that national water stress in China decreases after 2050, resulting in an even lower WSI in 2100 than 2005. In most basins, water scarcity is likely to be worst by 2035. Population decline, implementation of water conservation policies, and improvement in water use efficiency are responsible for the decline in water scarcity throughout China in the late 21st century. Although this study has incorporated climate-derived impacts on water supply, it does not account for *trans*-basin water diversion and the varying EFRs among basins. Moreover, certain policies, such as Chinese "three-child policy" may cause deviations from anticipated population change. Further studies that account for these policies may provide a more realistic assessment of changes in water stress.

CRediT authorship contribution statement

Yixin Sun: Conceptualization, Formal analysis, Methodology, Validation, Writing – original draft, Writing – review & editing. **Zhuotong Nan:** Conceptualization, Funding acquisition, Methodology, Resources, Supervision, Writing – original draft, Writing – review & editing. **Wendong Yang:** Methodology. **Longhui Li:** Funding acquisition, Resources.

Declaration of Competing Interest

The authors declare that they have no known competing financial interests or personal relationships that could have appeared to influence the work reported in this paper.

Data availability

I will share data on figshare and provide a doi to the manuscript.

Acknowledgments

The authors thank Inter-Sectoral Impact Model Intercomparison Project for providing future climate projection data, and the GCAM and Xanthos teams for providing the models.

Data statement

GCM projections were downloaded from the ISIMIP2b data set archive (https://www.isimip.org/gettingstarted/availability-input-data-isimip2b/, accessed January 4, 2022). Global population density maps were from HYDE (https://cmr.earthdata.nasa.gov/search/conc

epts/C1214613363-SCIOPS, accessed January 4, 2022) and SEDAC (https://sedac.ciesin.columbia.edu/data/collection/gpw-v4, accessed January 4, 2022). Gridded global maps of livestock were compiled by the Animal Production and Health Division in FAO from https://www.fao.org/livestock-systems/en/ (accessed January 4, 2022). The GCAM and Xanthos models used in this study can be accessed at https://github.com/JGCRI/gcam-core/releases (accessed January 4, 2022) and https://github.com/JGCRI/xanthos/releases (accessed January 4, 2022), respectively. Codes for spatial downscaling of water use and water withdrawals are available at https://github.com/JGCRI/tethys/releases (accessed January 4, 2022). Results of this integrated method are available at https://doi.org/10.6084/m9.figshare.22785104.

Funding sources

This work was supported by the grants of the National Key R&D Program of China (2017YFA0603603) and the National Natural Science Foundation of China (41971074).

Appendix A. Supplementary data

Supplementary data to this article can be found online at https://doi.org/10.1016/j.cliser.2023.100385.

References

Alcamo, J., Flörke, M., Märker, M., 2007. Future long-term changes in global water resources driven by socio-economic and climatic changes. Hydrol. Sci. J. 52 (2), 247–275. https://doi.org/10.1623/hysj.52.2.247.

Arnell, N.W., 2004. Climate change and global water resources: SRES emissions and socio-economic scenarios. Glob. Environ. Chang. 14 (1), 31–52. https://doi.org/10.1016/j.gloenvcha.2003.10.006.

Arnell, N.W., van Vuuren, D.P., Isaac, M., 2011. The implications of climate policy for the impacts of climate change on global water resources. Glob. Environ. Chang. 21 (2), 592–603. https://doi.org/10.1016/j.gloenvcha.2011.01.015.

Azar, C., Lindgren, K., Obersteiner, M., Riahi, K., van Vuuren, D.P., den Elzen, K.M.G.J., Möllersten, K., Larson, E.D., 2010. The feasibility of low CO2 concentration targets and the role of bio-energy with carbon capture and storage (BECCS). Clim. Change 100 (1), 195–202.

Boulange, J., Hanasaki, N., Yamazaki, D., Pokhrel, Y., 2021. Role of dams in reducing global flood exposure under climate change. Nat. Commun. 417 (12) https://doi.org/10.1038/s41467-020-20704-0.

Calvin, K., Bond-Lamberty, B., Clarke, L., Edmonds, J., Eom, J., Hartin, C., Kim, S., Kyle, P., Link, R., Moss, R., McJeon, H., Patel, P., Smith, S., Waldhoff, S., Wise, M., 2017. The SSP4: A world of deepening inequality. Glob. Environ. Chang. 42, 284–296.

Calvin, K., Patel, P., Clarke, L., Asrar, G., Bond-Lamberty, B., Cui, R.Y., Di Vittorio, A., Dorheim, K., Edmonds, J., Hartin, C., Hejazi, M., Horowitz, R., Iyer, G., Kyle, P., Kim, S., Link, R., McJeon, H., Smith, S.J., Snyder, A., Waldhoff, S., Wise, M., 2019. GCAM v5.1: Representing the linkages between energy, water, land, climate, and economic systems. Geosci. Model Dev. 12 (2), 677–698.

Clark, C.E., Horner, R.M., Harto, C.B., 2013. Life cycle water consumption for shale gas and conventional natural gas. Environ. Sci. Tech. 47 (20), 11829–11836. https://doi.org/10.1021/es4013855.

Dellink, R., Chateau, J., Lanzi, E., Magné, B., 2017. Long-term economic growth projections in the Shared Socioeconomic Pathways. Glob. Environ. Chang. 42, 200–214. https://doi.org/10.1016/J.GLOENVCHA.2015.06.004.

Derwent, R.G., Stevenson, D.S., Utembe, S.R., Jenkin, M.E., Khan, A.H., Shallcross, D.E., 2020. Global modelling studies of hydrogen and its isotopomers using STOCHEM-CRI: Likely radiative forcing consequences of a future hydrogen economy. Int. J. Hydrogen Energy 45 (15), 9211–9221. https://doi.org/10.1016/j.ijhydene.2020.01.125.

Eom, J., Clarke, L., Kim, S.H., Kyle, P., Patel, P., 2012. China's building energy demand: Long-term implications from a detailed assessment. Energy 46 (1), 405–419. https://doi.org/10.1016/j.energy.2012.08.009.

Ercin, A.E., Hoekstra, A.Y., 2014. Water footprint scenarios for 2050: A global analysis. Environ. Int. 64, 71–82. https://doi.org/10.1016/j.envint.2013.11.019.

Ercin, A.E., Hoekstra, A.Y., 2016. European water footprint scenarios for 2050. Water 8 (6), 226–240. https://doi.org/10.3390/w8060226.

Falkenmark, M., 1989. The massive water scarcity now threatening Africa - why isn't it being addressed? Ambio 18 (2), 112–118. https://doi.org/10.2307/4313541.

Falkenmark, M., Berntell, A., Jägerskog, A., Lundqvist, J., Matz, M., & Tropp, H. (2007). On the Verge of a New Water Scarcity: A Call for Good Governance and Human Ingenuity. *SIWI Policy Brief*, 20. Retrieved from http://dlc.dlib.indiana.edu/dlc/handle/10535/5086.

FAO. (2018). *AQUASTAT Database*. https://www.fao.org/aquastat/statistics/query/index.html accessed on [02/11/2021].

Feng, L., Chen, B., Hayat, T., Alsaedi, A., Ahmad, B., 2017. Dynamic forecasting of agricultural water footprint based on Markov Chain-a case study of the Heihe River Basin. Ecol. Model. 353, 150–157. https://doi.org/10.1016/j.ecolmodel.2016.11.002.

Fricko, O., Parkinson, S.C., Johnson, N., Strubegger, M., van Vliet, M.T., Riahi, K., 2016. Energy sector water use implications of a 2 °C climate policy. Environ. Res. Lett. 11 (3), 034011 https://doi.org/10.1088/1748-9326/11/3/034011.

Fricko, O., Havlik, P., Rogelj, J., Klimont, Z., Gusti, M., Johnson, N., Kolp, P., Strubegger, M., Valin, H., Amann, M., Ermolieva, T., Forsell, N., Herrero, M., Heyes, C., Kindermann, G., Krey, V., McCollum, D.L., Obersteiner, M., Pachauri, S., Rao, S., Schmid, E., Schoepp, W., Riahi, K., 2017. The marker quantification of the Shared Socioeconomic Pathway 2: A middle-of-the-road scenario for the 21st century. Glob. Environ. Chang. 42, 251–267.

Frieler, K., Lange, S., Piontek, F., Reyer, C.P.O., Schewe, J., Warszawski, L., et al., 2017. Assessing the impacts of 1.5 °C global warming - Simulation protocol of the Inter-Sectoral Impact Model Intercomparison Project (ISIMIP2b). Geosci. Model Dev. 10 (12), 4321–4345. https://doi.org/10.5194/gmd-10-4321-2017.

Ge, L., Xie, G., Li, S., Cheng, Y., Luo, Z., 2016. The analysis of water footprint of production and water stress in China. J. Resour. Ecol. 7 (5), 334–341. https://doi.org/10.5814/j.issn.1674-764x.2016.05.003.

Graham, N.T., Davies, E.G.R., Hejazi, M.I., Calvin, K., Kim, S.H., Helinski, L., Miralles-Wilhelm, F.R., Clarke, L., Kyle, P., Patel, P., Wise, M.A., Vernon, C.R., 2018. Water sector assumptions for the shared socioeconomic pathways in an integrated modeling framework. Water Resour. Res. 54 (9), 6423–6440.

Graham, N.T., Hejazi, M.I., Kim, S.H., Davies, E.G.R., Edmonds, J.A., Miralles-wilhelm, F., 2020a. Future changes in the trading of virtual water. Nat. Commun. 11, 1–7. https://doi.org/10.1038/s41467-020-17400-4.

Graham, N.T., Hejazi, M.I., Chen, M., Davies, E.G.R., Edmonds, J.A., Kim, S.H., Turner, S.W.D., Li, X., Vernon, C.R., Calvin, K., Miralles-Wilhelm, F., Clarke, L., Kyle, P., Link, R., Patel, P., Snyder, A.C., Wise, M.A., 2020b. Humans drive future water scarcity changes across all Shared Socioeconomic Pathways. Environ. Res. Lett. 15 (1), 014007.

Greve, P., Kahil, T., Mochizuki, J., Schinko, T., Satoh, Y., Burek, P., Fischer, G., Tramberend, S., Burtscher, R., Langan, S., Wada, Y., 2018. Global assessment of water challenges under uncertainty in water scarcity projections. Nat. Sustainability 1 (9), 486–494.

Hejazi, M., Edmonds, J., Clarke, L., Kyle, P., Davies, E., Chaturvedi, V., Wise, M., Patel, P., Eom, J., Calvin, K., Moss, R., Kim, S., 2014. Long-term global water projections using six socioeconomic scenarios in an integrated assessment modeling framework. *Technol. Forecast. Soc. Change* 81, 205–226.

Hejazi, M. I., Edmonds, J., Clarke, L., Kyle, P., Davies, E., Chaturvedi1, V., et al. (2013). Integrated assessment of global water scarcity over the 21st century – Part 2: Climate change mitigation policies. *Hydrol. Earth Syst. Sci.*, *10*(3), 3383–3425. https://doi.org/10.5194/hessd-10-3383-2013.

Hoekstra, A.Y., 2009. Human appropriation of natural capital: A comparison of ecological footprint and water footprint analysis. Ecol. Econ. 68 (7), 1963–1974. https://doi.org/10.1016/j.ecolecon.2008.06.021.

Hoekstra, A.Y., Mekonnen, M.M., Chapagain, A.K., Mathews, R.E., Richter, B.D., Añel, J.A., 2012. Global monthly water scarcity: Blue water footprints versus blue water availability. PLoS One 7 (2), e32688.

Hogeboom, R.J., De Bruin, D., Schyns, J.F., Krol, M.S., Hoekstra, A.Y., 2020. Capping human water footprints in the world's river basins. Earth's Future 8 (2). https://doi.org/10.1029/2019EF001363.

Huang, Z., Hejazi, M., Li, X., Tang, Q., Vernon, C., Leng, G., Liu, Y., Döll, P., Eisner, S., Gerten, D., Hanasaki, N., Wada, Y., 2018. Reconstruction of global gridded monthly sectoral water withdrawals for 1971–2010 and analysis of their spatiotemporal patterns. Hydrol. Earth Syst. Sci. 22 (4), 2117–2133.

Huang, Z., Liu, X., Sun, S., Tang, Y., Yuan, X., Tang, Q., 2021a. Global assessment of future sectoral water scarcity under adaptive inner-basin water allocation measures. Sci. Total Environ. 783, 146973 https://doi.org/10.1016/j.scitotenv.2021.146973.

Huang, Z., Yuan, X., Liu, X., 2021b. The key drivers for the changes in global water scarcity: water withdrawal versus water availability. J. Hydrol. 601, 126658.

IEA. (2021). Global Hydrogen Review 2021, October 21, https://www.iea.org/reports/global-hydrogen-review-2021.

Jiang, Y., 2009. China's water scarcity. J. Environ. Manage. 90 (11), 3185–3196. https://doi.org/10.1016/j.jenvman.2009.04.016.

Jiang, Y., 2015. China's water security: current status, emerging challenges and future prospects. Environ Sci Policy 54, 106–125. https://doi.org/10.1016/j.envsci.2015.06.006.

Kim, S.H., Edmonds, J., Lurz, J., Smith, S.J., Wise, M., 2006. The objECTS framework for integrated assessment: hybrid modeling of transportation. *Energy J.*, *SI* 2006 (01), 63–91. https://doi.org/10.5547/ISSN0195-6574-EJ-VolSI2006-NoSI2-4.

Kim, S.H., Hejazi, M., Liu, L., Calvin, K., Clarke, L., Edmonds, J., Kyle, P., Patel, P., Wise, M., Davies, E., 2016. Balancing global water availability and use at basin scale in an integrated assessment model. Clim. Change 136 (2), 217–231.

Konar, M., Reimer, J.J., Hussein, Z., Hanasaki, N., 2016. The water footprint of staple crop trade under climate and policy scenarios. Environ. Res. Lett. 11 (3), 035006.

Kriegler, E., Edmonds, J., Hallegatte, S., Ebi, K.L., Kram, T., Riahi, K., Winkler, H., van Vuuren, D.P., 2014. A new scenario framework for climate change research: The concept of shared climate policy assumptions. Clim. Change 122 (3), 401–414.

Kriegler, E., Bauer, N., Popp, A., Humpenöder, F., Leimbach, M., Strefler, J., Baumstark, L., Bodirsky, B.L., Hilaire, J., Klein, D., Mouratiadou, I., Weindl, I., Bertram, C., Dietrich, J.-P., Luderer, G., Pehl, M., Pietzcker, R., Piontek, F., Lotze-Campen, H., Biewald, A., Bonsch, M., Giannousakis, A., Kreidenweis, U., Müller, C., Rolinski, S., Schultes, A., Schwanitz, J., Stevanovic, M., Calvin, K., Emmerling, J.,

Fujimori, S., Edenhofer, O., 2017. Fossil-fueled development (SSP5): An energy and resource intensive scenario for the 21st century. Glob. Environ. Chang. 42, 297–315.
Kyle, P., Davies, E.G.R., Dooley, J.J., Smith, S.J., Clarke, L.E., Edmonds, J.A., Hejazi, M., 2013. Influence of climate change mitigation technology on global demands of water for electricity generation. Int. J. Greenhouse Gas Control 13, 112–123. https://doi.org/10.1016/J.IJGGC.2012.12.006.
Lehner, B., Liermann, C.R., Revenga, C., Vörösmarty, C., Fekete, B., Crouzet, P., Döll, P., Endejan, M., Frenken, K., Magome, J., Nilsson, C., Robertson, J.C., Rödel, R., Sindorf, N., Wisser, D., 2011. High-resolution mapping of the world's reservoirs and dams for sustainable river-flow management. Front. Ecol. Environ. 9 (9), 494–502.
Li, X., Vernon, C.R., Hejazi, M.I., Link, R.P., Feng, L., Liu, Y., Rauchenstein, L.T., 2017. Xanthos – a global hydrologic model. J. Open Res. Software 5 (1), 21.
Li, X., Vernon, C.R., Hejazi, M.I., Link, R.P., Huang, Z., Liu, L., Feng, L., 2018. Tethys - A Python package for spatial and temporal downscaling of global water withdrawals. J. Open Res. Software 6 (1). https://doi.org/10.5334/jors.197.
Liu, Y., Hejazi, M., Li, H., Zhang, X., Leng, G., 2018. A hydrological emulator for global applications–HE v1.0.0. Geosci. Model Dev. 11 (3), 1077–1092. https://doi.org/10.5194/gmd-11-1077-2018.
Liu, J., Yang, H., Gosling, S.N., Kummu, M., Flörke, M., Pfister, S., Hanasaki, N., Wada, Y., Zhang, X., Zheng, C., Alcamo, J., Oki, T., 2017. Water scarcity assessments in the past, present, and future. Earth's Future 5 (6), 545–559.
Madhu, K., Pauliuk, S., Dhathri, S., Creutzig, F., 2021. Understanding environmental trade-offs and resource demand of direct air capture technologies through comparative life-cycle assessment. Nat. Energy 6 (11), 1035–1044. https://doi.org/10.1038/s41560-021-00922-6.
McSweeney, C.F., Jones, R.G., 2016. How representative is the spread of climate projections from the 5 CMIP5 GCMs used in ISI-MIP? Clim. Serv. 1, 24–29. https://doi.org/10.1016/J.CLISER.2016.02.001.
Mekonnen, M.M., Hoekstra, A.Y., 2016. Sustainability: Four billion people facing severe water scarcity. Sci. Adv. 2 (2), 1–4. https://doi.org/10.1126/sciadv.1500323.
Mendelsohn, R., Nordhaus, W.D., Shaw, D., 1994. The impact of global warming on agriculture: a Ricardian analysis. Am. Econ. Rev. 84 (4), 753–771. https://doi.org/10.2307/2118029.
Ministry of Water Resources of China, 2005. China Water Resources Bulletin. China Water & Power Press, Beijing.
Ministry of Water Resources of China, 2010. China Water Resources Bulletin. China Water & Power Press, Beijing.
Ministry of Water Resources of China, 2015. China Water Resources Bulletin. China Water & Power Press, Beijing.
Ministry of Water Resources of China, 2020a. China Water Resources Bulletin. China Water & Power Press, Beijing.
Ministry of Water Resources of China, 2020b. China Water Statistical Yearbook. China Water & Power Press, Beijing.
Munia, H.A., Guillaume, J.H.A., Wada, Y., Veldkamp, T., Virkki, V., Kummu, M., 2020. Future transboundary water stress and its drivers under climate change: a global study. Earth's Future 8 (7). https://doi.org/10.1029/2019ef001321.
Muratoglu, A., 2020. Assessment of wheat's water footprint and virtual water trade: a case study for Turkey. Ecological Process 9, 13. https://doi.org/10.1186/s13717-020-0217-1.
O'Neill, B.C., Kriegler, E., Ebi, K.L., Kemp-Benedict, E., Riahi, K., Rothman, D.S., van Ruijven, B.J., van Vuuren, D.P., Birkmann, J., Kok, K., Levy, M., Solecki, W., 2017. The roads ahead: Narratives for shared socioeconomic pathways describing world futures in the 21st century. Glob. Environ. Chang. 42, 169–180.
Orlowsky, B., Hoekstra, A.Y., Gudmundsson, L., Seneviratne, S.I., 2014. Today ' s virtual water consumption and trade under future water scarcity. Environ. Res. Lett. 9 (7), 074007.
Prudhomme, C., Giuntoli, I., Robinson, E.L., Clark, D.B., Arnell, N.W., Dankers, R., Fekete, B.M., Franssen, W., Gerten, D., Gosling, S.N., Hagemann, S., Hannah, D.M., Kim, H., Masaki, Y., Satoh, Y., Stacke, T., Wada, Y., Wisser, D., 2014. Hydrological droughts in the 21st century, hotspots and uncertainties from a global multimodel ensemble experiment. Proc. Natl. Acad. Sci. 111 (9), 3262–3267.
Reinecke, R., Müller Schmied, H., Trautmann, T., Andersen, L.S., Burek, P., Flörke, M., Gosling, S.N., Grillakis, M., Hanasaki, N., Koutroulis, A., Pokhrel, Y., Thiery, W., Wada, Y., Yusuke, S., Döll, P., 2021. Uncertainty of simulated groundwater recharge at different global warming levels: A global-scale multi-model ensemble study. Hydrol. Earth Syst. Sci. 25 (2), 787–810.
Riahi, K., van Vuuren, D.P., Kriegler, E., Edmonds, J., O'Neill, B.C., Fujimori, S., Bauer, N., Calvin, K., Dellink, R., Fricko, O., Lutz, W., Popp, A., Cuaresma, J.C., Kc, S., Leimbach, M., Jiang, L., Kram, T., Rao, S., Emmerling, J., Ebi, K., Hasegawa, T., Havlik, P., Humpenöder, F., Da Silva, L.A., Smith, S., Stehfest, E., Bosetti, V., Eom, J., Gernaat, D., Masui, T., Rogelj, J., Strefler, J., Drouet, L., Krey, V., Luderer, G., Harmsen, M., Takahashi, K., Baumstark, L., Doelman, J.C., Kainuma, M., Klimont, Z., Marangoni, G., Lotze-Campen, H., Obersteiner, M., Tabeau, A., Tavoni, M., 2017. The Shared Socioeconomic Pathways and their energy, land use, and greenhouse gas emissions implications: An overview. Glob. Environ. Chang. 42, 153–168.
Samir, K.C., Wolfgang, L., 2017. The human core of the shared socioeconomic pathways: Population scenarios by age, sex and level of education for all countries to 2100. Glob. Environ. Chang. 42, 181–192. https://doi.org/10.1016/J.GLOENVCHA.2014.06.004.
Schewe, J., Heinke, J., Gerten, D., Haddeland, I., Arnell, N.W., Clark, D.B., Dankers, R., Eisner, S., Fekete, B.M., Colón-González, F.J., Gosling, S.N., Kim, H., Liu, X., Masaki, Y., Portmann, F.T., Satoh, Y., Stacke, T., Tang, Q., Wada, Y., Wisser, D., Albrecht, T., Frieler, K., Piontek, F., Warszawski, L., Kabat, P., 2014. Multimodel assessment of water scarcity under climate change. Proc. Natl. Acad. Sci. U.S.A. 111 (9), 3245–3250.
Séférian, R., Rocher, M., Guivarch, C., Colin, J., 2018. Constraints on biomass energy deployment in mitigation pathways: the case of water scarcity. Environ. Res. Lett. 13 (5), 054011 https://doi.org/10.1088/1748-9326/AABCD7.
Smolenaars, W.J., Dhaubanjar, S., Jamil, M.K., Lutz, A., Immerzeel, W., Ludwig, F., Biemans, H., 2022. Future upstream water consumption and its impact on downstream water availability in the transboundary Indus Basin. Hydrol. Earth Syst. Sci. 26 (4), 861–883. https://doi.org/10.5194/hess-26-861-2022.
Tian, X., Sarkis, J., Geng, Y., Qian, Y., Gao, C., Bleischwitz, R., 2018. Evolution of China ' s water footprint and virtual water trade : A global trade assessment. Environ. Int. 121, 178–188. https://doi.org/10.1016/j.envint.2018.09.011.
van Vuuren, D.P., Kriegler, E., O'Neill, B.C., Ebi, K.L., Riahi, K., Carter, T.R., Edmonds, J., Hallegatte, S., Kram, T., Mathur, R., Winkler, H., 2014. A new scenario framework for Climate Change Research: scenario matrix architecture. Clim. Change 122 (3), 373–386.
Veldkamp, T.I.E., Wada, Y., Aerts, J.C.J.H., Döll, P., Gosling, S.N., Liu, J., Masaki, Y., Oki, T., Ostberg, S., Pokhrel, Y., Satoh, Y., Kim, H., Ward, P.J., 2017. Water scarcity hotspots travel downstream due to human interventions in the 20th and 21st century. Nat. Commun. 8 (1) https://doi.org/10.1038/ncomms15697.
Vernon, C.R., Hejazi, M.I., Turner, S.W.D., Liu, Y., Braun, C.J., Li, X., Link, R.P., 2019. A global hydrologic framework to accelerate scientific discovery. Journal of Open Research Software 7 (1), 1.
Voisin, N., Li, H., Ward, D., Huang, M., Wigmosta, M., Leung, L.R., 2013. On an improved sub-regional water resources management representation for integration into earth system models. Hydrol. Earth Syst. Sci. 17 (9), 3605–3622. https://doi.org/10.5194/hess-17-3605-2013.
Wang, G.Q., Zhang, J.Y., 2015. Variation of water resources in the Huang-huai-hai areas and adaptive strategies to climate change. Quat. Int. 380–381, 180–186. https://doi.org/10.1016/j.quaint.2015.02.005.
Wu, Z., Zhang, Y., Hua, Y., Ye, Q., Xu, L., Wang, S., 2020. An improved system dynamics model to evaluate regional water scarcity from a virtual water perspective: A case study of Henan Province. China. *Sustainability* 12 (18), 7517. https://doi.org/10.3390/su12187517.
Xie, P., Zhuo, L.a., Yang, X.i., Huang, H., Gao, X., Wu, P., 2020. Spatial-temporal variations in blue and green water resources, water footprints and water scarcities in a large river basin: A case for the Yellow River basin. J. Hydrol. 590, 125222.
Xu, X., Zhang, Y., Chen, Y., 2020. Projecting China's future water footprint under the shared socio-economic pathways. J. Environ. Manage. 260, 110102.
Yin, Y., Wang, L., Wang, Z., Tang, Q., Piao, S., Chen, D., Xia, J., Conradt, T., Liu, J., Wada, Y., Cai, X., Xie, Z., Duan, Q., Li, X., Zhou, J., Zhang, J., 2020. Quantifying water scarcity in Northern China Within the Context of Climatic and Societal Changes and South-to-North Water Diversion. Earth's Future 8 (8). https://doi.org/10.1029/2020EF001492.
Zeng, Z., Liu, J., Koeneman, P.H., Zarate, E., Hoekstra, A.Y., 2012. Assessing water footprint at river basin level : a case study for the Heihe River Basin in northwest China. Hydrol. Earth Syst. Sci. 16 (8), 2771–2781. https://doi.org/10.5194/hess-16-2771-2012.
Zhang, C., Zhao, Y.i., Shi, C., Chiu, Y.-h., 2021. Can China achieve its water use peaking in 2030? A scenario analysis based on LMDI and Monte Carlo method. J. Clean. Prod. 278, 123214.
Zhao, Y., Li, H., Liu, H., Wang, L., He, G., Wang, H., 2021. The law of growth:prediction of peak water consumption in China. J. Hydrol. Eng. 52 (2), 129–141. https://doi.org/10.13243/j.cnki.slxb.20200457.
Zhou, F., Bo, Y., Ciais, P., Dumas, P., Tang, Q., Wang, X., Liu, J., Zheng, C., Polcher, J., Yin, Z., Guimberteau, M., Peng, S., Ottle, C., Zhao, X., Zhao, J., Tan, Q., Chen, L., Shen, H., Yang, H., Piao, S., Wang, H., Wada, Y., 2020. Deceleration of China's human water use and its key drivers. Proc. Natl. Acad. Sci. U.S.A. 117 (14), 7702–7711.